Greener and Efficient Epoxidation of 1,5-Hexadiene with *tert*-Butyl Hydroperoxide (TBHP) as an Oxidising Reagent in the Presence of Polybenzimidazole Supported Mo(VI) Catalyst

Md Masud Rana Bhuiyan [1], Misbahu Ladan Mohammed [2] and Basudeb Saha [1,*]

[1] School of Engineering, Lancaster University, Lancaster LA1 4YW, UK; m.m.bhuiyan@lancaster.ac.uk

[2] Department of Energy and Applied Chemistry, Usmanu Danfodiyo University, Sokoto, 840004, Nigeria; misbahu.ladan@udusok.edu.ng

* Correspondence: b.saha@lancaster.ac.uk

Abstract: Alkene epoxidation with TBHP as an oxidising reagent using heterogeneous Mo(VI) catalyst is an environmentally friendly process since it eliminates acid waste and chlorinated by-products often associated with the conventional industrial method that uses stoichiometric peracid such as peracetic acid and m-chloroperbenzoic acid. Polybenzimidazole supported Mo(VI) complex, i.e., PBI.Mo has been successfully prepared, characterised and assessed for the epoxidation of 1,5-hexadiene in the presence of *tert*-butyl hydroperoxide (TBHP) as an oxidising reagent. A quadratic polynomial model has been developed, demonstrating the yield of 1,2-epoxy-5-hexene in four independent variables. The effects of different parameters such as reaction temperature, feed mole ratio of 1,5-hexadiene to TBHP, catalyst loading, and reaction time were studied. Response surface methodology (RSM) using Box-Behnken Design (BBD) was employed to study the interaction effect of different variables on the reaction response. This study presents the optimization of 1,5-hexadiene epoxidation in a batch reactor using TBHP as an oxidant and a polymer-supported Mo(VI) catalyst.

Keywords: alkene epoxidation; heterogeneous catalysis; *tert*-butyl hydroperoxide (TBHP); polymer supported Mo(VI) catalyst; 1,5-hexadiene; response surface methodology (RSM).

1. Introduction

Alkene epoxidation has been established as an important process for chemical synthesis as the resultant epoxide acts as a raw material or intermediate that can be transformed into many useful substances such as plasticizers, perfumes, and epoxy resins [1]. The reaction occurs by direct oxidation of two adjacent carbon atoms from alkene in the presence of oxidising reagents [2,3]. The versatile nature of epoxides is due to the high reactivity of the three-membered ring in their structure [4]. Furthermore, a number of epoxides show great importance in biological activity and are very useful in the development of drugs, agrochemicals, and additives [5]. For the synthesis of taxol, a powerful anti-cancer drug [6], and for the synthesis of hydrogels that are applied in tissue replacement [7], 1,2-epoxy-5-hexene epoxide is one of the important epoxides used. Additionally, it has been reported that 1,2-epoxy-5-hexene incorporated polysiloxane can be actively employed as high brightness light emitting diodes (LED) encapsulant [8].

The production of ethylene and propylene oxides are some of the notable industrial epoxidations that are carried out in the liquid phase with an alkyl hydroperoxide as a source of oxygen [9,10]. Although molecular oxygen and hydrogen peroxide are probably the most eco-friendly oxidants since they both produce water as their only by-product, their major limitation as oxidising reagents in epoxidation is low product selectivity [11,12]. The conventional epoxidation method uses stoichiometric peracids, such as peracetic acid and *m*-chloroperbenzoic acid or chlorohydrin, as oxidising agents in batch

reactions [13,14]. However, the application of these reagents is not environmentally friendly as peracids produce an equivalent amount of acid waste while chlorohydrin yields chlorinated by-products [14]. Another notable liquid phase epoxidation is known as the Halcon process, catalysed by homogeneous molybdenum(VI) or heterogeneous Ti(IV) supported on SiO_2 [15]. Homogeneous catalysed epoxidation processes are not economically viable for industrial applications due to corrosion and deposition on the reactor, in addition to major requirements in terms of work-up, product isolation, and purification procedures [16].

There has been a considerable amount of research work on epoxidation reactions carried out with a broad range of catalytic materials by immobilisation of catalytically active metal species on organic or inorganic materials, such as silica [17,18], zeolites [19,20], alumina [21,22], ion-exchange resins [23,24], polymers [25–27], and metal-organic frameworks [28]. However, polymer-supported heterogeneous catalysts have been successfully used for the synthesis of epoxides in recent years in the presence of *tert*-butyl hydroperoxide as an oxidant and have shown high catalytic activity and product selectivity [29–31]. Polymers have gained attention as suitable supports for catalysts as they are stable, inert, nontoxic, and insoluble [32–35]. However, despite numerous published works on polymer-supported Mo(VI) catalysts in the epoxidation of different alkene substrates, there appears to be no report yet on the epoxidation of 1,5-hexadiene with *tert*-butyl hydroperoxide as an oxidising reagent in the presence of a polymer-supported Mo(VI) catalyst.

In this process, an efficient and selective polybenzimidazole supported molybdenum (VI) complex (PBI.Mo) has been used as a catalyst for the batch epoxidation of 1,5-hexadiene. This system is free of solvents and uses the environmentally friendly TBHP as an oxidant. Experiments have been carried out to study the effects of different parameters, including reaction temperature, feed molar ratio of alkene to TBHP and catalyst loading, on the yield of 1,2-epoxy-5-hexene to optimise the reaction conditions in a classical batch reactor. A quadratic polynomial model has been developed using Response Surface Methodology (RSM). Box–Behnken Design (BBD) has been employed to study the interaction between the effects of different variables on the conversion of alkene and the yield of the epoxide product. This study presents the optimization of 1,5-hexadiene epoxidation using TBHP as an oxidant and a polymer-supported Mo(VI) complex as a catalyst in a batch reactor.

## 2. Materials and Methods

2.1. Materials

All chemicals used during catalyst preparation were purchased from Sigma-Aldrich Co., Ltd., and gas chromatography (GC) was used to verify the purity of the chemicals. Microporous polybenzimidazole (PBI) resin beads were supplied by Celanese Corporation, USA. The preparation of the polybenzimidazole-supported Mo(VI) complex, i.e., PBI.Mo catalyst was carried out using sodium hydroxide (purum p.a., ≥98%), deionised water, acetone, molybdenyl acetylacetonate ($MoO_2(acac)_2$) (99%) and toluene (anhydrous, 99.8%). Reactants involved in this study were 1,5-hexadiene (97%) and *tert*-butyl hydroperoxide (TBHP) solution in water (70% (*w/w*)). The quantification of samples collected from the reactor was carried out using the internal standard method in the GC, and *iso*-octane (anhydrous, 99.8%) was used as an internal standard.

2.2. Preparation of Polymer-Supported Mo(VI) Catalyst

A NaOH solution (1M) was used to stir wet polybenzimidazole (PBI) resin beads. PBI was pre-treated by stirring overnight. The polymer beads were then washed with deionised water until the pH of the washing liquid turned neutral; then acetone was used to wash the polymer beads. Thereafter, the beads were collected and dried under a vacuum at 40 °C. The treated PBI resin (5 g) was refluxed with excess $MoO_2(acac)_2$ (17.68 g) in

anhydrous toluene for a period of 4 days. The ratio of $MoO_2(acac)_2$ to the functional ligand used was 2:1. The reaction was carried out in a 0.25 L reactor at ~105 °C and stirred gently with the overhead mechanical device at ~150 rpm. The PBI beads changed colour from brown to green. The PBI.Mo catalyst particles were separated by filtration at the end of the reaction, and excess $MoO_2(acac)_2$ was removed by exhaustive extraction with acetone. The green colour disappeared by washing upon repeated introduction of fresh solvent until the solution remained colourless. PBI.Mo catalyst particles were collected and dried in a vacuum oven at 40 °C. As shown in the proposed reaction mechanism (Scheme 1), the bidentate ligand (acetylacetonate ion) binds itself to the molybdenum with the two oxygen atoms by electron delocalisation, while the metal is attached to the resin by the electron pairs of nitrogen. The FTIR spectrum showed the incorporation of Mo centres in the resin due to the presence of Mo=O and Mo-O-Mo vibrations characteristics.
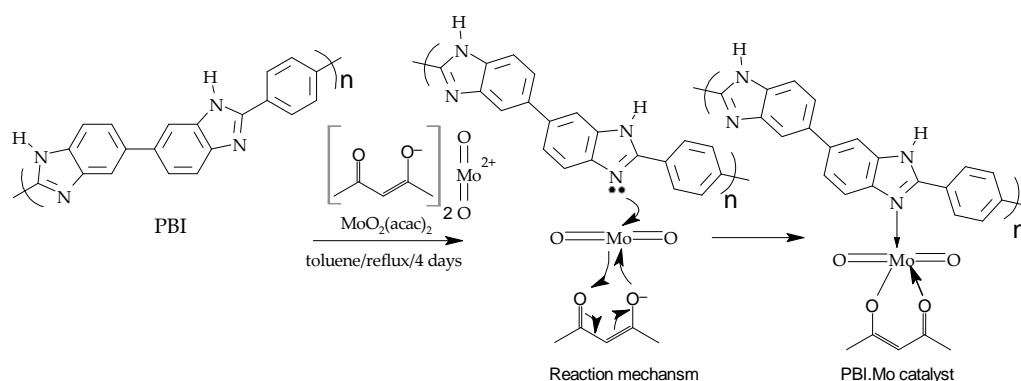
Scheme 1. Reaction mechanism for the synthesis of polybenzimidazole supported Mo(VI) (PBI.Mo) complex.

2.3. Characterisation of Polymer-Supported Mo(VI) Catalyst

The molybdenum content of the prepared catalysts was analysed using a PerkinElmer NexION 350D spectrophotometer. The Brunauer–Emmett–Teller (BET) surface area, pore volume, and pore diameter were determined by the nitrogen adsorption and desorption methods using Micromeritics Gemini VII. The particle size measurement was performed with a Malvern Mastersizer. The properties of the prepared PBI.Mo catalyst are summarised in Table 1. The FTIR spectrum of the PBI.Mo catalyst was observed on a Thermal Nicolet Avectar 370 DTGS equipped with a smart orbit accessory. A finely grounded sample of the catalyst was placed on the sample stage and the spectrum was recorded with the aid of OMINIC software. The PBI.Mo spectrum showed Mo=O and Mo-O-Mo vibrations characteristics with adsorption bands of around ~690 cm^{-1} to ~900 cm^{-1}. The morphology of PBI.Mo catalyst particles was examined using a PEMTRON PS-230 scanning electron microscope (SEM). The catalyst was dried in a vacuum oven before analysis to remove any moisture present in the catalyst. Then it was mounted on the gold-coated specimen holder and the accelerating voltage for SEM analysis was set to ~8.0 Kv. The SEM image of the PBI.Mo catalyst shows a well-dispersed spherical smooth surface with negligible mechanical damage to the sample, and has a well-dispersed spherical smooth surface, a property of macroporous polymeric resins.

Table 1. Properties of polybenzimidazole supported Mo(VI) (i.e., PBI.Mo) catalyst.

Catalyst Properties	Values obtained
BET surface area	18.44 m^2/g
Pore volume	0.021986 cm^3/g
Mo loading (mmol Mo g^{-1} resin)	0.825
Average Pore diameter	21.595 Å
Average particle size	210–295 μm

2.4. Batch Epoxidation Studies

Batch epoxidation of 1,5-hexadiene with TBHP as an oxidant in the presence of a polymer-supported Mo(VI) catalyst was conducted in a 0.25 L jacketed four-neck glass reactor. The batch reactor was equipped with a condenser, an overhead stirrer, a digital thermocouple, a sampling point, and a water bath as shown in Figure 1.
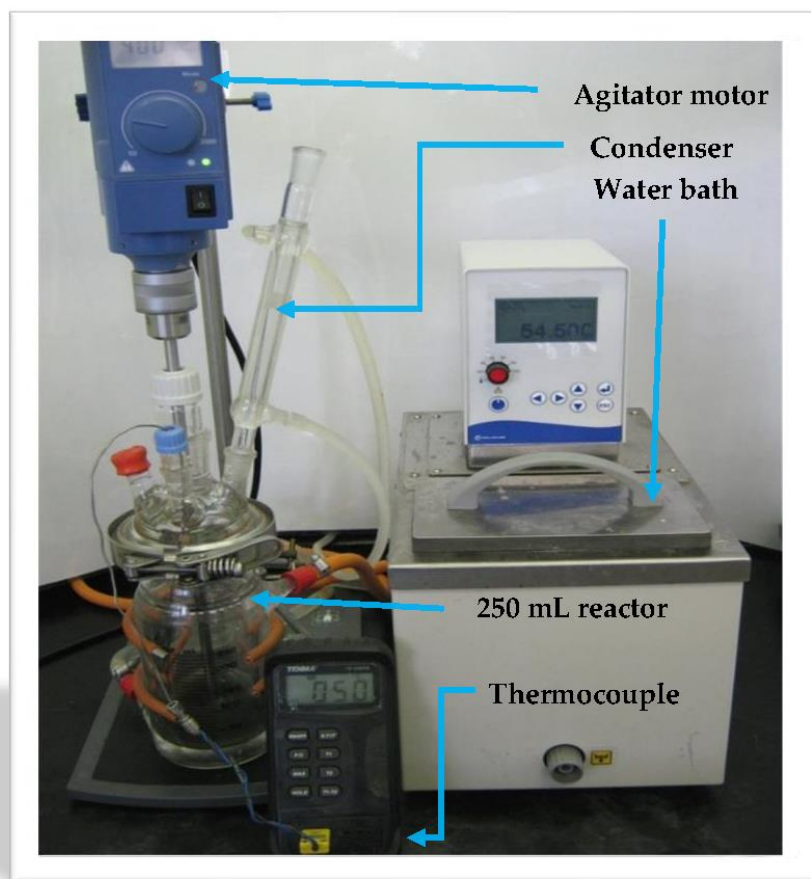

Figure 1. Experimental set-up of batch epoxidation studies.

Known quantities of 1,5-hexadiene and TBHP were weighted out and introduced into the reactor vessel and stirring was started at the desired rate (400 rpm). A feed molar ratio (FMR) of 1,5-hexadiene to TBHP of 1:1–10:1 was selected for charging the reactor. Heating to the reaction mixture was supplied through a water bath via the reactor jacket and monitored by a digital thermocouple. The temperature of the reaction mixture was allowed to reach the desired value, i.e., 333 K–353 K, and was maintained in the range of ± 2 K throughout the batch experiment. A known amount of catalyst (0.15–0.6 mol% Mo loading) was added to the reactor when the reaction mixture reached a constant desired temperature. The reaction scheme for the epoxidation of 1,5-hexadiene with TBHP as an oxidant is shown in Scheme 2.
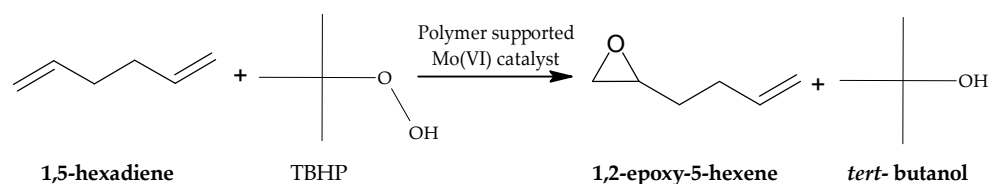
Scheme 2. Epoxidation of 1,5-hexadiene with TBHP catalysed by the PBI.Mo catalyst.

A sample was collected after the catalyst was added and the time was noted as zero time, i.e., t = 0. Subsequent samples were taken from the reaction mixture at specific time intervals and recorded. The samples collected were analysed using Shimadzu GC-2014 gas chromatography (GC).

2.5. Method of Analysis

A specific quantity of internal standard (*iso*-octane) was added to a number of samples with known concentrations of the components in the product mixture and analysed using Shimadzu GC-2014 gas chromatography. The instrument was fitted with a flame ionisation detector (FID), an auto-injector, and a 30 m long Econo-CapTM-5 (ECTM-5) capillary column. Helium was used as a carrier gas. The flow rate of carrier gas was 1 mL min^{-1}. The split ratio was 100:1 and an injection volume of 0.5 μL was selected. The temperature for both the injector and the detector was 523 K. The oven temperature was maintained at 313 K for 4 min after the sample was injected and ramped from 313 K to 498 K at a rate of 20 °C per minute. Each sample takes ~13 min to be analysed by GC, and the temperature was cooled back to 313 K before starting the next run.

2.6. Experimental Design

Response surface methodology (RSM) is a multivariate method that can develop a model representing the reaction-dependent response function of the independent variables studied experimentally [36]. RSM has been developed to determine the optimum conditions for epoxide production by studying the relationship between each variable and the response yield. The experimental runs have been operated based on four independent variables, including reaction feed molar ratio of 1,5-hexadiene to TBHP, reaction temperature, catalyst loading, and reaction time, which were labelled as A, B, C, and D, respectively. Three levels for each variable have been coded as −1, 0, +1 as shown in Table 2. Box-Behnken Design (BBD) is one of the RSM techniques that is used to study the main effect of process variables on the response. It also studies the effect of the variables' interactions on the response. The yield of 1,2-epoxy-5-hexene has been selected as the response for this study. The experiments were completed in a randomised order to minimise the effect of unexplained inconsistency in the response. Twenty-nine runs were conducted randomly, and their responses were calculated from the experimental results [37].

Table 2. Experimental design variables and their coded levels.

Factors	Code	Levels		
		−1	0	1
FMR	A	2.5	6.25	10
Temperature (K)	B	333	343	353
Catalyst loading (mol%)	C	0.15	0.375	0.6
Time (min)	D	0	60	120

2.7. Statistical Analysis

The mathematical model was defined using the general quadratic model as shown in Equation (1).

$$Y = b_o + \sum_{i=1}^{n} b_i x_i + \sum_{i=1}^{n} b_{ii} x_i^2 + \sum_{i=1}^{n-1} \sum_{j>1}^{n} b_{ij} x_i x_j + \varepsilon \tag{1}$$

where Y is the predicted response (i.e., yield of 1,2-epoxy-5-hexene), b_o is the model coefficient constant, b_i, b_{ii}, b_{ij}, are coefficients for the intercept of linear, quadratic, and interactive terms, respectively, while x_i, x_i are independent variables ($i \neq j$), n is a number of independent variables and ε is the random error.

The adequacy of the predicted models was checked by several statistical validations, including the coefficient of correlation (R^2), adjusted coefficient of determination (R^2_{adj})

and the predicted coefficient of determination (R^2_{pred}). The statistical significance of the predicted models was analysed by ANOVA using Fisher's test, i.e., F-value and p-value, at a 95% confidence interval. The Design Expert 11 software (Stat-Ease Inc., Minneapolis, MN, USA) was used to perform the initial experimental design, model prediction, statistical analysis, and optimisation.

3. Results and Discussion

3.1. Development of Regression Model and Adequacy Checking

The predicted model was examined for adequacy in reporting any errors associated with the assumptions of normality. After evaluating the yield of 1,2-epoxy-5-hexene (reaction response) for each run, the response analysis using BBD has been applied. The Design Expert software generated an equation of regression representing an empirical relationship between the response variable and the reaction parameters. By fitting the experimental results, the generic quadratic equation shown in Equation (1) was used to obtain a model of polynomial regression. The polynomial equation is shown in Equation (2).

$$Y = 53.27 - 2.50A + 1.45B + 4.44C + 9.17D - 2.81AB + 1.59AC - 0.1600AD + 1.86BC - 2.26BD + 0.5300CD + 1.63A^2 - 0.9042\ B^2 + 1.05C^2 - 10.25D^2 \tag{2}$$

where, Y represents the dependent variable (yield of epoxide), while A, B, C, and D represent the independent variables i.e., feed molar ratio, reaction temperature, catalyst loading, and reaction time, respectively. Furthermore, AB, AC, AD, BC, BD, and CD represent the interaction between independent variables. Finally, A^2, B^2, C^2 and D^2 represent the excess of each independent variable.

The developed models have demonstrated the effects of each independent variable, variable interactions, and excess of each variable on the response. The positive sign of each variable coefficient represents the synergetic effect of the variable on the response. However, the negative sign represents the antagonistic effect on the response.

ANOVA has been applied to examine the significance of the model parameters at a 95% confidence level. The significance of each parameter has been determined by F-test and p-value. The higher the value of the F-test and the smaller the p-value, the more significant the corresponding parameter [38].

ANOVA has been used to validate the RSM model coefficient using the F-test and p-value, these values have been concluded as 15.69 and <0.0001, respectively, as shown in Table 3 which proves that the developed quadratic model is statistically significant with 95% confidence level. The lack-of-fit analysis is one of the adequacies checking techniques that measure the failure of the regression model to represent the experimental data points [39].

The lack-of-fit value of the model has been concluded to be 0.456 (not significant), which illustrates that the model has been representing most of the experimental data successfully. The determination coefficient values, R^2 and R^2_{adj}, which measure the reliability of the model fitting, have been calculated to be 0.9401 and 0.8802, respectively. The adequate precision is 13.98, which is desirable and ensures the model fits the experimental data.

Table 3. Analysis of variance for response surface developed model.

Source	Sum of squares	df	Mean square	F-value	p-value	Significance
Model	2230.55	14	159.33	15.69	< 0.0001	Significant
A-FMR	75.00	1	75.00	7.39	0.0167	Significant
B-Temperature	25.35	1	25.35	2.50	0.1364	Not significant
C-Catalyst Loading	236.47	1	236.47	23.29	0.0003	significant
D-time	1008.52	1	1008.52	99.34	< 0.0001	significant
AB	31.58	1	31.58	3.11	0.0996	not significant
AC	10.18	1	10.18	1.00	0.3337	not significant
AD	0.1024	1	0.1024	0.0101	0.9214	not significant
BC	13.80	1	13.80	1.36	0.2631	not significant
BD	20.39	1	20.39	2.01	0.1783	not significant
CD	1.12	1	1.12	0.1107	0.7443	not significant
A^2	17.20	1	17.20	1.69	0.2141	not significant
B^2	5.30	1	5.30	0.5223	0.4817	not significant
C^2	7.11	1	7.11	0.7005	0.4167	not significant
D^2	681.87	1	681.87	67.17	< 0.0001	significant
Residual	142.13	14	10.15			
Lack of Fit	107.22	10	10.72	1.23	0.4557	not significant
Pure Error	34.91	4	8.73			
Cor Total	2372.68	28				

The model's performance has been observed using different techniques. A plot of the predicted versus the experimental result of the yield of epoxide in Figure 2 showed a high correlation and reasonable agreement. The good estimate for the response values from the model is concluded from the similarity between the predicted and actual experimental results as shown in Figure 2. In addition, a plot of residual distribution versus predicted response has been presented to check the fitting performance of the model, as shown in Figure 3. A residual value is defined as the difference between predicted and experimental values of the response variable. The plot confirms that the quadratic model adequately represents the experimental data as the distribution is not following a specified trend concerning the predicted values of the response variable. Moreover, the perturbation plot represents the effect of each variable on the reaction response as shown in Figure 4. The curvature of the variables from the centre point indicates the significance of each variable, which confirms the statistical results obtained from ANOVA as shown in Table 3. The sharp curvature of the independent variables, e.g., catalyst loading (C) and reaction time (D), indicates their significance as seen from the ANOVA results. It also represents the effect of the feed molar ratio. The plot indicates that catalyst loading and time have progressively increasing effects on the yield of epoxide until reaching the central point.
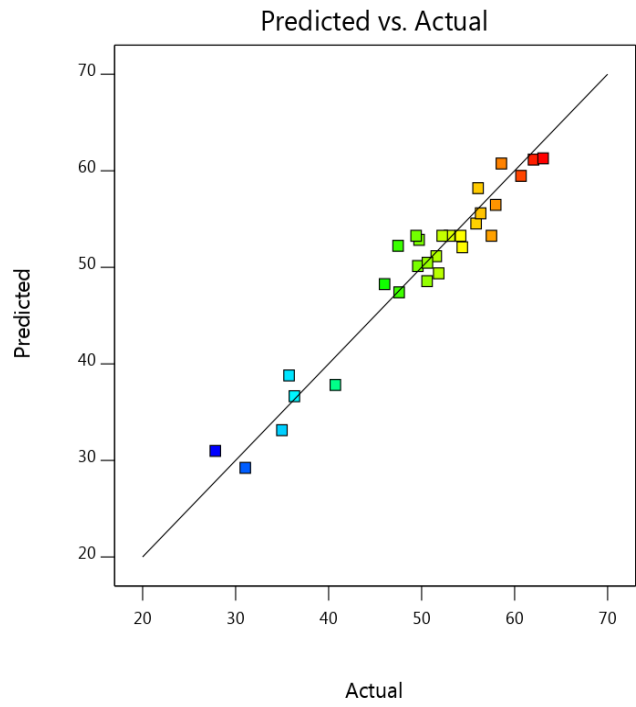
Figure 2. Actual experimental data versus predicted model.
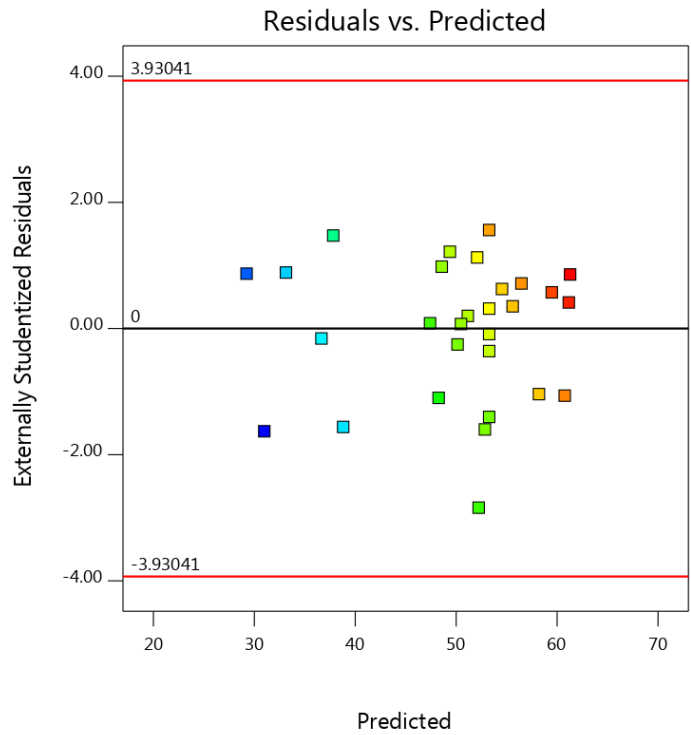
Figure 3. Residual versus predicted response.

Design-Expert® Software
Factor Coding: Actual

Yiled (%)

Actual Factors
A: FMR = 6.25
B: Temperature = 343
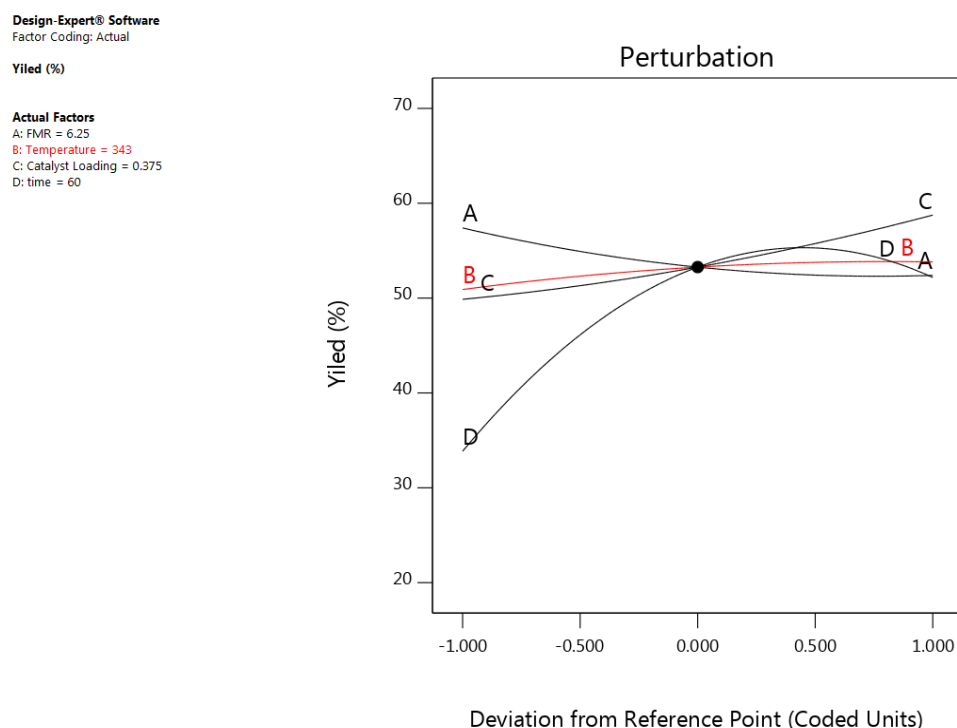C: Catalyst Loading = 0.375
D: time = 60

Figure 4. The perturbation plot represents the effect of each variable on the reaction response.

3.2. Effect of Process Variables and Their Interactions

The effect of each independent process variable on the process response was investigated in this section. In addition, the interactive effect was highlighted in the responses of various independent variables. The 3D-surface plots of epoxide yield versus two independent variables' interaction are displayed. The two remaining independent variables were kept at their centre points constant in each plot.

3.2.1. Effect of Feed Molar Ratio (FMR)

In most catalysed processes of alkene epoxidation, reactions are performed with a substantial excess of alkene to avoid over-oxidation and achieve high oxidant conversion and high epoxide yield. As a result, several batch experiments were conducted to study the effect of different alkene to TBHP feed molar ratios on epoxide yield.

Experimental runs have been carried out at feed molar ratios of alkene to TBHP between 2.5:1 and 10:1 to study the effect on the yield of the epoxide. Based on the ANOVA results presented in Table 3, the FMR parameter shows a significant effect on the process response. The experiments conducted at 2.5:1 and 10:1 molar ratios of 1,5-hexadiene to TBHP gave 60.7% and 55.6% yields of 1,2-epoxy-5-hexene, respectively, at 60 min (Figure 5). As shown in Figure 5, the influence of FMR of 1,5-hexadiene to TBHP was more noticeable when a stoichiometric ratio (2.5:1) was used, as there was no significant difference in the rate of epoxidation when the feed molar ratio of 1,5-hexadiene to TBHP was increased from 2.5:1 to 10:1. A similar observation was reported for PBI.Mo catalysed epoxidation of 1-hexene and 4-vinyl-1-cyclohexene with TBHP, where an increase in the FMR of alkene to TBHP led to a decrease in the rate of formation of the corresponding epoxide [40]. Similar results for 1-octene epoxidation with TBHP in the presence of a polymer-supported Mo(VI) catalyst were observed when the molar ratio of 1-octene to TBHP was increased from 5:1 to 10:1 [41].
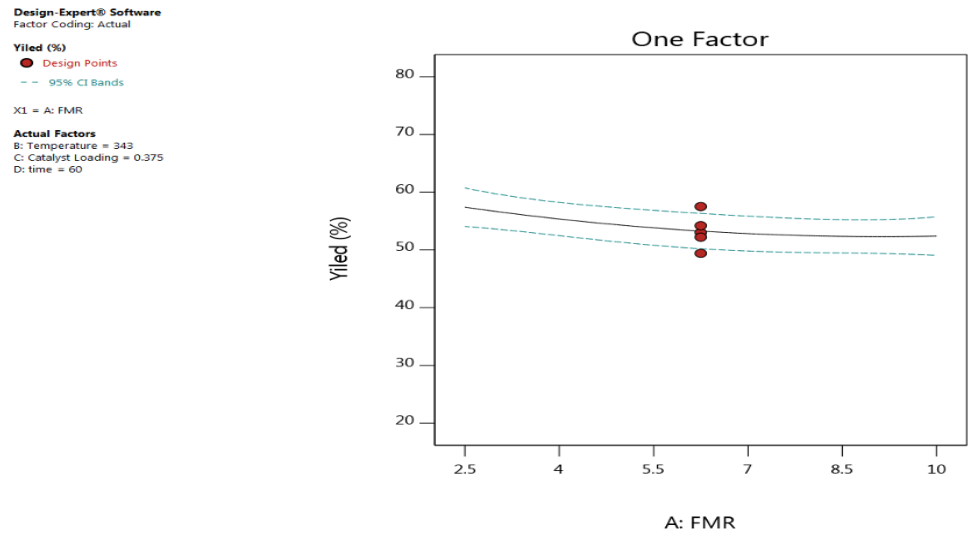
Figure 5. The effect of feed molar ratio on the yield of 1,2-epoxy-5-hexene.

Based on the results of this study (Figure 6), it can be concluded that at 76 min, the optimal molar feed ratio of 1,5-hexadiene to TBHP was 2.76:1 at 348 K temperature and 0.56 mol% catalyst loading.
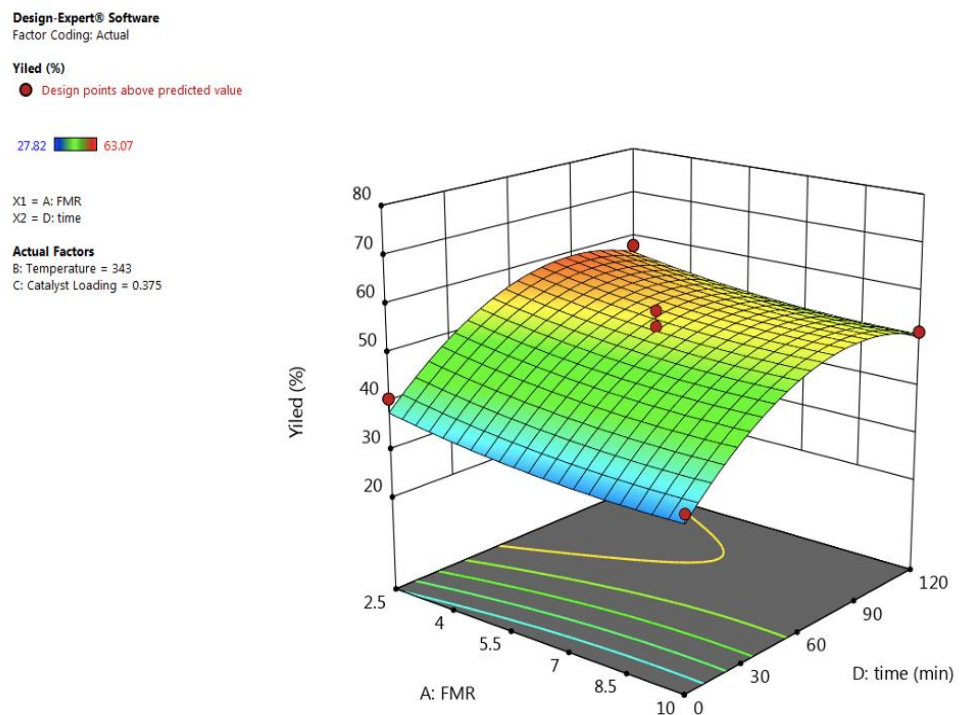

Figure 6. 3-D graph showing the effect of feed molar ratio and time on the yield of 1,2-epoxy-5-hexene.

3.2.2. Effect of Reaction Temperature

The epoxidation of 1,5-hexadiene with TBHP has been carried out at 333 K, 343 K, and 353 K to study the effect of reaction temperature on the yield of 1,2-epoxy-5-hexene.

The ANOVA results presented in Table 3 show no significant effect of reaction temperature on the process response. It is clearly shown in Figure 7 that at 60 min the yield of 1,2-epoxy-5-hexene was 54.25% and 57.1% at 333 K and 353 K, respectively. The 3-D

surface graph (Figure 8) shows that the yield of epoxide at 0.35 mol% catalyst loading was 50.73% and 53.23% at 333 K and 353 K, respectively. This was due to the distinct exothermic effect. Mohammed (2015) [40] reported a similar result for the epoxidation of 4-vinyl-1-cyclohexene with TBHP where the reaction reached equilibrium within the first 5 min.

It can be concluded that at 0.56 mol% catalyst loading, 348 K is the preferred reaction temperature for the epoxidation of 1,5-hexadiene at 76 min and the feed molar ratio of 1,5-hexadiene to TBHP is 2.76:1.
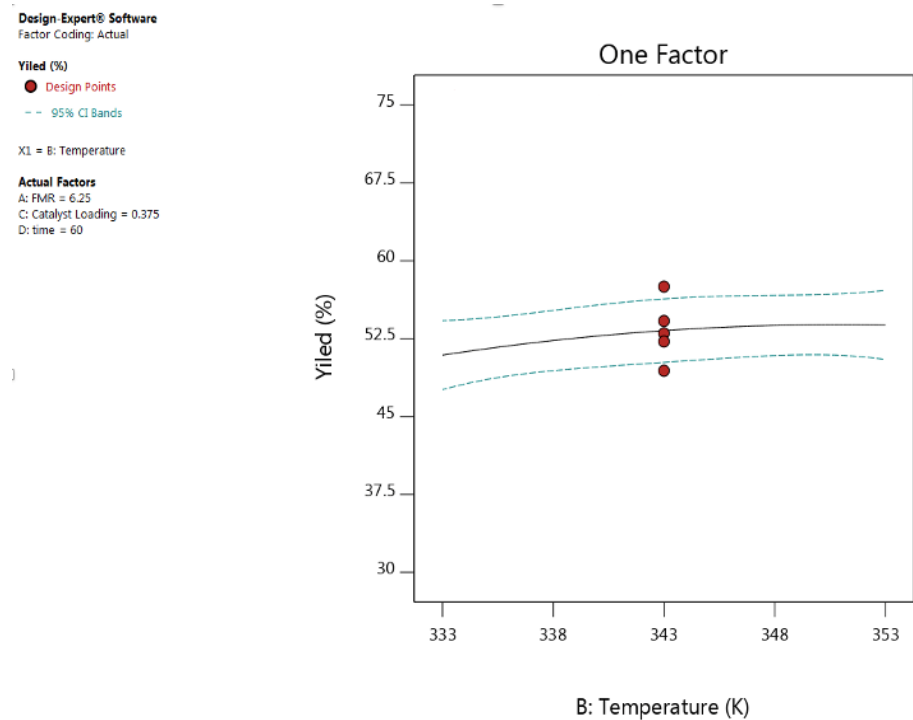

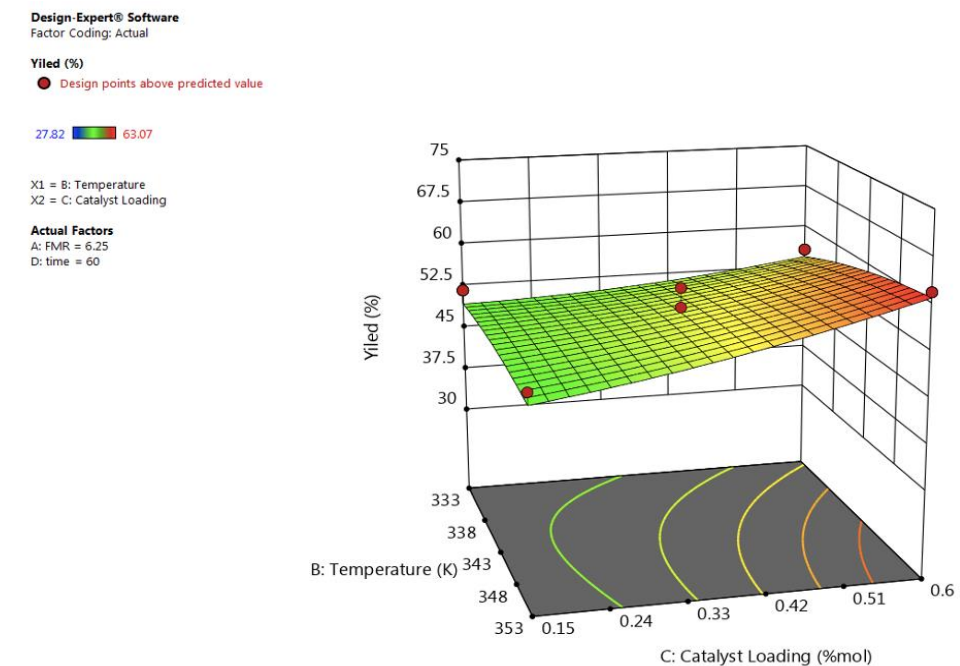**Figure 7.** The effect of reaction temperature on the yield of 1,2-epoxy-5-hexene.

Figure 8. 3-D graph showing the effect of temperature and catalyst loading on the yield of 1,2-epoxy-5-hexene.

3.2.3. Effect of Catalyst Loading

An increase in catalyst loading increases the number of active sites per unit volume of the reactor, leading to an increase in the yield of epoxides. Thus, the effect of catalyst loading (i.e., mole ratio of Mo to TBHP x 100%) for epoxidation of 1,5-hexadiene with TBHP was investigated by conducting batch experiments using 0.15 mol% Mo, 0.375 mol% Mo, and 0.6 mol% Mo catalyst loading. Based on the ANOVA results presented in Table 3, the catalyst loading parameter shows a significant effect on the process response. It is clearly shown in Figure 9 that a positive correlation exists between catalyst loading and epoxide yield within the temperature range between 333 K and 353 K. The yield of 1,2-epoxy-5-hexene at 60 min was ~49% and ~59% for reactions conducted at 0.15 mol% Mo and 0.6 mol% Mo, respectively, while the FMR of 1,5-hexadiene to TBHP was 6.25:1. Figure 10 shows that the yield of epoxide at feed molar ratio of 1,5-hexadiene to TBHP of 9.6:1 was ~47% and ~57% at 0.15 mol% Mo and 0.5 mol% Mo, respectively. However, it was observed that for 1-hexene epoxidation in the presence of a PBI.Mo catalyst [30], catalyst loading of 0.15 mol% Mo provided a sufficient active site for the reaction, thus, an increase in catalyst loading beyond 0.15 mol% Mo (i.e., 0.3–0.6 mol% Mo) had a negligible effect on the rate of formation of 1,2-epoxyhexane. It can be concluded that 0.56 mol% catalyst loading is the preferred catalyst loading at 348 K for the epoxidation of 1,5-hexadiene at 76 min and the feed molar ratio of 1,5-hexadiene to TBHP is 2.76:1.
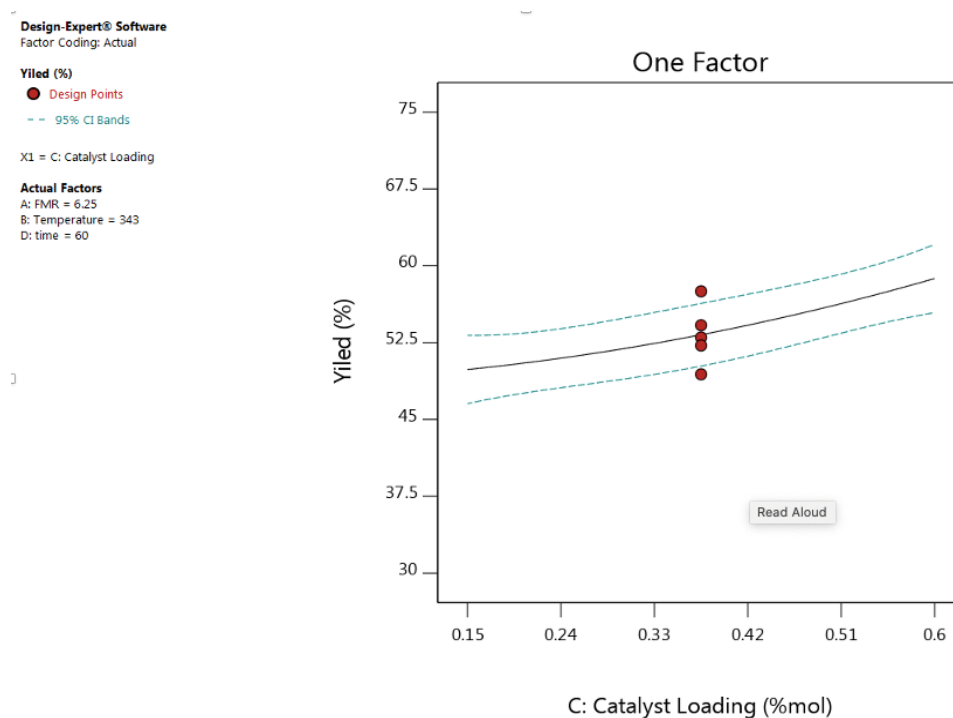

Figure 9. The effect of catalyst loading on the yield of 1,2-epoxy-5-hexene.
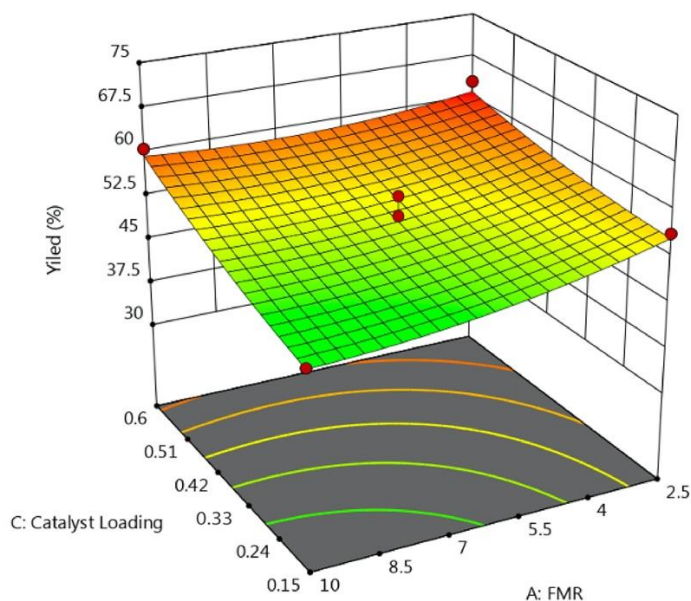
Figure 10. 3-D graph showing the effect of catalyst loading and FMR on the yield of 1,2-epoxy-5-hexene.

3.2.4. Effect of Reaction Time

In this study, a sample was collected after the catalyst was added and the time was noted as zero time, i.e., t = 0. Subsequent samples were taken from the reaction mixture at specific time intervals and recorded. Based on the ANOVA results presented in Table 3, the reaction time parameter shows a significant effect on the process response. The result shows a fairly large increase in the rate of epoxidation with an increase in time. As shown in Figure 11, the yield of 1,2-epoxy-5-hexene increases by increasing the time between 0 min and 87 min. Figure 11 also reveals that at 343 K, the yield of 1.2-epoxy-5-hexene was 30% and 58% at 0 min and 80 min, respectively. The yield of epoxide starts to decrease after 87 min. The 3-D surface graph (Figure 12) shows that the yield of epoxide at 0.4 mol% catalyst loading was 40%, 56%, and 53% at 12 min, 88 min, and 118 min, respectively. It can be concluded that 76 min is the preferred reaction time at 348 K for the epoxidation of 1,5-hexadiene at 0.56 mol% catalyst loading and the feed molar ratio of 1,5-hexadiene to TBHP is 2.76:1.
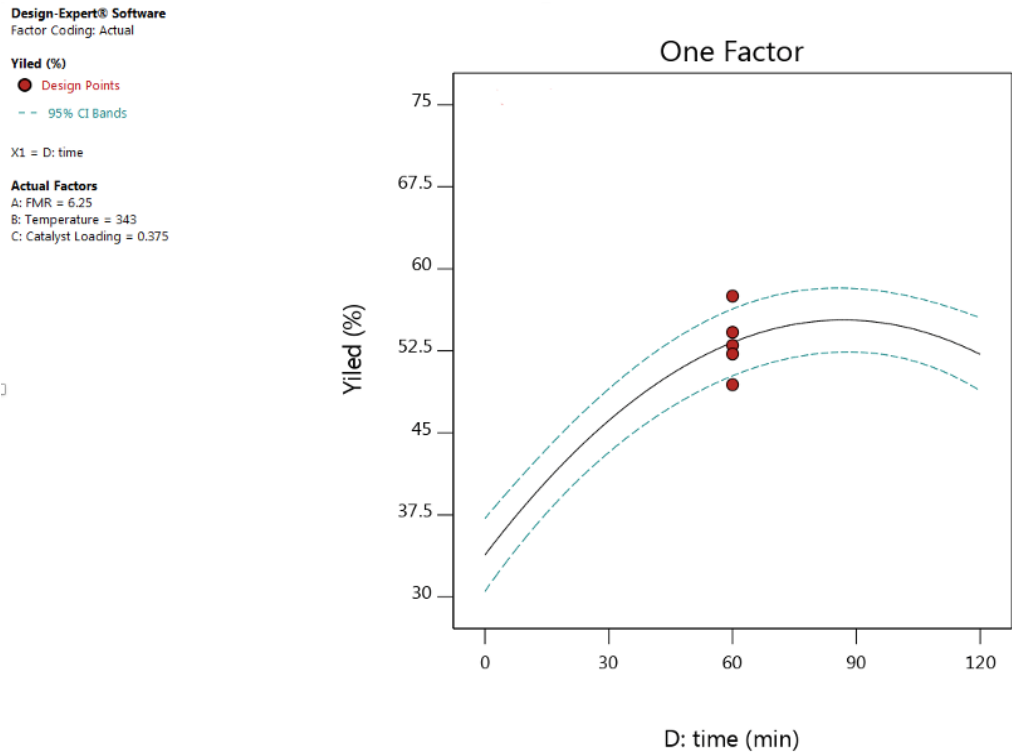
Figure 11. The effect of reaction time on the yield of 1,2-epoxy-5-hexene.
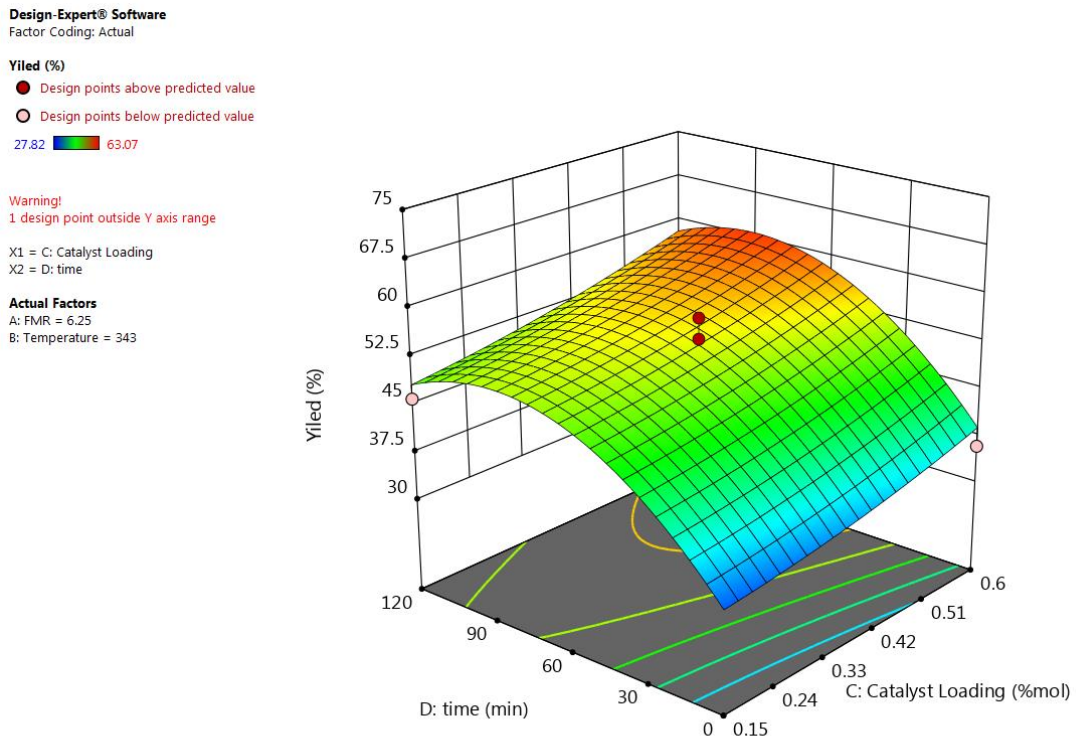

Figure 12. 3-D graph showing the effect of reaction time and catalyst loading on the yield of 1,2-epoxy-5-hexene.

3.3. Optimisation Study of Reaction Variables

An optimisation process of the epoxidation reaction has been carried out to find the optimum values for the independent variables affecting the dependent response variable. Design Expert Software has been used to develop the numerical optimisation step by combining the desirability of each independent variable into a single value and then searching for optimum values for the response goals. Accordingly, to determine the optimum conditions of the independent variables, a set of targets must be defined in the software to guide the optimisation process [38].

The dependent response variable (yield of 1,2-epoxy-5-hexene) has been set to be maximised to achieve the highest yield. The numerical optimisation technique concluded that the maximum yield that can be reached is 64.2% at a feed molar ratio of 2.76:1, a reaction temperature of 348 K, a 0.56 mol% catalyst loading, and a reaction time of 76 min. An optimisation study of PBI.Mo catalysed epoxidation of 1-hexene using an artificial neural network (ANN) revealed that reaction temperature has the most pronounced effect on the yield of 1,2-epoxyhexane, while the influence of catalyst loading or the feed mole ratio of 1-hexene to TBHP is not very distinct [30].

3.4. Optimum Conditions Validation

To validate the optimal response values of the predicted quadratic equation, experiments have been performed at optimum conditions, i.e., feed molar ratio of 2.76:1, reaction temperature of 348 K, 0.56 mol% catalyst loading, and reaction time of 76 min. The experimental results showed a similar response value to the predicted optimal response of 62.03% with a relative error of 3.5%. The relative error can be affected by the temperature variation during the reaction.

4. Conclusions

The polymer-supported Mo(VI) (PBI.Mo) complex has been prepared, characterised, and assessed as a catalyst for the epoxidation of 1,5-hexadiene in a batch reactor using TBHP as an oxidant. The PBI.Mo catalyst has been proven to be active for batch reactions. Reaction variables and operating conditions of the reaction have been optimised. A quadratic polynomial model has been developed to demonstrate the yield of 1,2-epoxy-5-hexene in four independent variables. Batch epoxidation experiments were carried out to analyse the effects of temperature, the molar ratio of reactants, and catalyst loading on the yield of 1,2-epoxy-5-hexene.

The optimum conditions observed for the maximum yield of 1,2-epoxy-5 hexene are a 2.76:1 feed molar ratio of 1,5-hexadiene to TBHP, 348 K reaction temperature, 76 min reaction time, and 0.56 mol% catalyst loading. The optimisation result has been validated experimentally, resulting in an epoxide yield of 62.03%, which shows the adequacy of the predicted optimum conditions with a 3.5% relative error from the experimental results. This study demonstrates that polymer-supported Mo(VI) (PBI.Mo complex) could be used as an effective catalyst for a greener and more efficient epoxidation of 1,5-hexadiene with *tert*-butyl hydroperoxide (TBHP) as an oxidising reagent.

References

1. Grivani, G.; Tangestaninejad, S.; Habibi, M.H.; Mirkhani, V. Epoxidation of alkenes by a highly reusable and efficient polymer-supported molybdenum carbonyl catalyst. *Catal. Commun*. **2005**, *6*, 375–378.

2. Mohammed, M.L.; Saha, B. Recent Advances in Greener and Energy Efficient Alkene Epoxidation Processes. *Energies* **2022**, *15*, 2858.

3. Saha, B.; Ambroziak, K.; Sherrington, D.C.; Mbeleck, R. Epoxidation Process. European Patent Number EP2459545B1, 28 February 2019.

4. Schaus, S.E.; Brandes, B.D.; Larrow, J.F.; Tokunaga, M.; Hansen, K.B.; Gould, A.E.; Furrow, M.E.; Jacobsen, E.N. Highly Selective Hydrolytic Kinetic Resolution of Terminal Epoxides Catalyzed by Chiral (salen)CoIII Complexes. Practical Synthesis of Enantioenriched Terminal Epoxides and 1,2-Diols. *J. Am. Chem. Soc.* **2002**, *124*, 1307–1315.

5. Grivani, G.; Tangestaninejad, S.; Habibi, M.H.; Mirkhani, V.; Moghadam, M. Epoxidation of alkenes by a readily prepared and highly active and reusable heterogeneous molybdenum-based catalyst. *Appl. Catal. A Gen*. **2006**, *299*, 131–136.

6. García, R.; Martínez, M.; Aracil, J. Enzymatic esterification of an acid with an epoxide using immobilized lipase from Mucor miehei as catalyst: Optimization of the yield and isomeric excess of ester by statistical analysis. *J. Ind. Microbiol. Biotechnol.* **2002**, *28*, 173–179.

7. Bader, R.A. Synthesis and viscoelastic characterization of novel hydrogels generated via photopolymerization of 1,2-epoxy-5-hexene modified poly(vinyl alcohol) for use in tissue replacement. *Acta Biomater*. **2008**, *4*, 967–975.

8. Yahya, S.N.; Lin, C.K.; Ramli, M.R.; Jaafar, M.; Ahmad, Z. Effect of cross-link density on optoelectronic properties of thermally cured 1,2-epoxy-5-hexene incorporated polysiloxane. *Mater. Des*. **2013**, *47*, 416–423.

9. Tangestaninejad, S.; Mirkhani, V.; Moghadam, M.; Grivani, G. Readily prepared heterogeneous molybdenum-based catalysts as highly recoverable, reusable and active catalysts for alkene epoxidation. *Catal. Commun*. **2007**, *8*, 839–844.

10. Miller, M.M.; Sherrington, D.C. Polybenzimidazole-supported molybdenum(VI) propene epoxidation catalyst. *J. Chem. Soc. Chem. Commun*. **1994**, *1*, 55–56.

11. Shi, Z.-Q.; Jiao, L.-X.; Sun, J.; Chen, Z.-B.; Chen, Y.-Z.; Zhu, X.-H.; Zhou, J.-H.; Zhou, X.-C.; Li, X.-Z.; Li, R. Cobalt nanoparticles in hollow mesoporous spheres as a highly efficient and rapid magnetically separable catalyst for selective epoxidation of styrene with molecular oxygen. *RSC Adv*. **2014**, *4*, 47–53.

12. Vondran, J.; Pela, J.; Palczewski, D.; Skiborowski, M.; Seidensticker, T. Curse and Blessing–The Role of Water in the Homogeneously Ru-Catalyzed Epoxidation of Technical Grade Methyl Oleate. *ACS Sustain. Chem. Eng.* **2021**, *9*, 11469–11478.

13. Santacesaria, E.; Tesser, R.; Di Serio, M.; Turco, R.; Russo, V.; Verde, D. A biphasic model describing soybean oil epoxidation with H_2O_2 in a fed-batch reactor. *Chem. Eng. J.* **2011**, *173*, 198–209.

14. Bechtold, K. Versatile and Vexing: The Many Uses and Hazards of Peracetic Acid. Synergist 2016. Available online: https://synergist.aiha.org/201612-peracetic-acid-uses-and-hazards (accessed on 12 April 2022).

15. Kollar, J. Epoxidation Process. U.S. Patent Number US53617966A, 11 July 1967.

16. Salavati-Niasari, M.; Esmaeili, E.; Seyghalkar, H.; Bazarganipour, M. Cobalt(II) Schiff base complex on multi-wall carbon nanotubes (MWNTs) by covalently grafted method: Synthesis, characterization and liquid phase epoxidation of cyclohexene by air. *Inorg. Chim. Acta* **2011**, *375*, 11–19.

17. Shen, Y.; Jiang, P.; Zhang, J.; Bian, G.; Zhang, P.; Dong, Y.; Zhang, W. Highly dispersed molybdenum incorporated hollow mesoporous silica spheres as an efficient catalyst on epoxidation of olefins. *Mol. Catal.* **2017**, *433*, 212–223.

18. Bisio, C.; Gallo, A.; Psaro, R.; Tiozzo, C.; Guidotti, M.; Carniato, F. Tungstenocene-grafted silica catalysts for the selective epoxidation of alkenes. *Appl. Catal. A Gen.* **2019**, *581*, 133–142.

19. Cai, L.; Chen, C.; Wang, W.; Gao, X.; Kuang, X.; Jiang, Y.; Li, L.; Wu, G. Acid-free epoxidation of soybean oil with hydrogen peroxide to epoxidized soybean oil over titanium silicalite-1 zeolite supported cadmium catalysts. *Ind. Eng. Chem. Res.* **2020**, *91*, 191–200.

20. Wu, Z.; He, Z.; Zhou, D.; Yang, Y.; Lu, X.; Xia, Q. One-step synthesis of bi-functional zeolite catalyst with highly exposed octahedral Co for efficient epoxidation of bulky cycloalkenes. *Mater. Lett.* **2020**, *280*, 128549.

21. Lueangchaichaweng, W.; Singh, B.; Mandelli, D.; Carvalho, W.A.; Fiorilli, S.; Pescarmona, P.P. High surface area, nanostructured boehmite and alumina catalysts: Synthesis and application in the sustainable epoxidation of alkenes. *Appl. Catal. A Gen*. **2019**, *571*, 180–187.

22. Mikolajska, E.; Calvino-Casilda, V.; Bañares, M.A. Real-time Raman monitoring of liquid-phase cyclohexene epoxidation over alumina-supported vanadium and phosphorous catalysts. *Appl. Catal. A Gen*. **2012**, *421–422*, 164–171.

23. Borugadda, V.B.; Goud, V.V. Epoxidation of Castor Oil Fatty Acid Methyl Esters (COFAME) as a Lubricant base Stock Using Heterogeneous Ion-exchange Resin (IR-120) as a Catalyst. *Energy Procedia* **2014**, *54*, 75–84.

24. Peng, C.; Lu, X.H.; Ma, X.T.; Shen, Y.; Wei, C.C.; He, J.; Zhou, D.; Xia, Q.H. Highly efficient epoxidation of cyclohexene with aqueous H_2O_2 over powdered anion-resin supported solid catalysts. *J. Mol. Catal. A-Chem.* **2016**, *423*, 393–399.

25. Mohammed, M.L.; Mbeleck, R.; Patel, D.; Sherrington, D.C.; Saha, B. Greener route to 4-vinyl-1-cyclohexane 1,2-epoxide synthesis using batch and continuous reactors. *Green Process. Synth.* **2014**, *3*, 411–418.

26. Saha, B.; Ambroziak, K.; Sherrington, D.C.; Mbeleck, R. Liquid Phase Epoxidation Process. U.S. Patent Number U.S. 9,248,942 B2, 2 February 2016.

27. Mohammadikish, M.; Yarahmadi, S.; Molla, F. A new water-insoluble coordination polymer as efficient dye adsorbent and olefin epoxidation catalyst. *J. Environ. Manag.* **2020**, *254*, 109784.

28. Otake, K.-i.; Ahn, S.; Knapp, J.; Hupp, J.T.; Notestein, J.M.; Farha, O.K. Vapor-Phase Cyclohexene Epoxidation by Single-Ion Fe(III) Sites in Metal–Organic Frameworks. *Inorg. Chem.* **2021**, *60*, 2457–2463.

29. Mbeleck, R.; Mohammed, M.L.; Ambroziak, K.; Sherrington, D.C.; Saha, B. Efficient epoxidation of cyclododecene and dodecene catalysed by polybenzimidazole supported Mo(VI) complex. *Catal. Today* **2015**, *256*, 287–293.

30. Mohammed, M.L.; Patel, D.; Mbeleck, R.; Niyogi, D.; Sherrington, D.C.; Saha, B. Optimisation of alkene epoxidation catalysed by polymer supported Mo(VI) complexes and application of artificial neural network for the prediction of catalytic performances. *Appl. Catal. A-Gen.* **2013**, *466*, 142–152.

31. Mohammed, M.L.; Saha, B. Greener and sustainable approach for the synthesis of commercially important epoxide building blocks using polymer-supported Mo(VI) complexes as catalysts. In *Ion Exchange and Solvent Extraction*, 1st ed.; SenGupta, A.K., Ed.; CRC Press: Boca Raton, FL, USA.; Taylor & Francis Group LLC: Milton Park, UK, 2016; p 33.

32. Saha, B.; Ambroziak, K.; Sherrington, D.C.; Mbeleck, R. A Continuous Process for the Liquid Phase Epoxidation of an Olefinic Compound. Indian Patent No. 295846, 17 April 2018.

33. Saha, B. *Catalytic Reactors*; Walter de Gruyter GmbH & Co KG: Berlin, Germany, 2015.

34. Saha, B.; Ambroziak, K.; Sherrington, D.C.; Mbeleck, R. A Permeable Particle Container. Chinese Patent No. ZL 201410840925.7, 7 December 2016.

35. Mbeleck, R.; Ambroziak, K.; Saha, B.; Sherrington, D.C. Stability and recycling of polymer-supported Mo(VI) alkene epoxidation catalysts. *React. Funct. Polym.* **2007**, *67*, 1448–1457.

36. Aboelazayem, O.; Gadalla, M.; Saha, B. Biodiesel production from waste cooking oil via supercritical methanol: Optimisation and reactor simulation. *Renew. Energ.* **2018**, *124*, 144–154.

37. Onyenkeadi, V.; Aboelazayem, O.; Saha, B. Systematic multivariate optimisation of butylene carbonate synthesis via CO_2 utilisation using graphene-inorganic nanocomposite catalysts. *Catal. Today* **2020**, *346*, 10–22.

38. El-Gendy, N.S.; Deriase, S.F.; Hamdy, A. The Optimization of Biodiesel Production from Waste Frying Corn Oil Using Snails Shells as a Catalyst. *Energ. Source Part A.* **2014**, *36*, 623–637.

39. Yuan, J.; Huang, J.; Wu, G.; Tong, J.; Xie, G.-Y.; Duan, J.-a.; Qin, M. Multiple responses optimization of ultrasonic-assisted extraction by response surface methodology (RSM) for rapid analysis of bioactive compounds in the flower head of Chrysanthemum morifolium Ramat. *Ind. Crop Prod.* **2015**, *74*, 192–199.

40. Mohammed, M.L.; Mbeleck, R.; Patel, D.; Niyogi, D.; Sherrington, D.C.; Saha, B. Greener and efficient epoxidation of 4-vinyl-1-cyclohexene with polystyrene 2-(aminomethyl)pyridine supported Mo(VI) catalyst in batch and continuous reactors. *Chem. Eng. Res. Des.* **2015**, *94*, 194–203.

41. Ambroziak, K.; Mbeleck, R.; He, Y.; Saha, B.; Sherrington, D.C. Investigation of batch alkene epoxidations catalyzed by polymer-supported Mo(VI) complexes. *Ind. Eng. Chem. Res.* **2009**, *48*, 3293–3302.